

**TOXIC ELEMENT NICKEL ANALYSIS IN WATER SAMPLES USING A
PORTABLE NEUTRON GENERATOR BASED PGNAAS SETUP**



PHYS – 503 GRADUATE LABORATORY (Term 172)

Student Name: SYED SHAHEEN SHAH

Student ID: g201709190

Supervisor: PROF. AKHTAR ABBAS NAQVI

Department of Physics

King Fahd University of Petroleum and Minerals

(Dated: 06/03/2018)

Table of Contents

List of Figures	II
List of Tables	II
Abstract	III
1 Introduction.....	1
2 Objectives	3
3 Experimental setup.....	3
3.1 Energy Calibration of detector using Cs-137 and Co-60 Sources	5
4 Prompt Gamma Ray Studies.....	7
4.1 Background Spectrum.....	7
4.2 Nickel-Contaminated Water Sample Spectrum	7
5 Results and Discussion	8
5.1 Minimum Detection Limit of Nickel in Water Samples.....	10
6 Conclusion	11
7 Acknowledgements.....	11
8 References.....	11

List of Figures

Figure 1. The process of neutron captured by target nucleus followed by the emission of prompt gamma ray, delayed gamma ray, and beta particle.	2
Figure 2: Schematic representation of the MP320 portable neutron generator based PGNAAs setup.	4
Figure 3: Detector $CeBr_3$ intrinsic activity spectrum.	5
Figure 4: Full spectrum of (a) Cs-137 and (b) Co-60 for calibration with $CeBr_3$ detector.	6
Figure 5: Energy calibration curve of the $CeBr_3$ detector using Cs-137 and Co-60 standard samples.	6
Figure 6: Detector $CeBr_3$ intrinsic activity spectrum.	7
Figure 7: Superimposed spectra of the background (dotted line) and nickel (solid line)..	8
Figure 8: Normalized Spectra for the three nickel samples with 2.7, 5.0, and 6.5 wt% nickel concentration.	9
Figure 9: Difference spectra for three nickel samples with 2.7, 5.0, and 6.5 wt% nickel concentration.	9
Figure 10: Concentration calibration plot of gamma-ray intensity vs. nickel concentrations (wt%).	10

List of Tables

Table 1: List of nickel samples used for analysis.	4
Table 2: MDC values for the two peaks of nickel and combined.	11

Abstract

The Minimum Detectable Concentration (MDC) of a large cylindrical $76\text{ mm} \times 76\text{ mm}$ (diameter \times height) cerium tribromide ($CeBr_3$) detector was measured for prompt gamma rays. The Prompt Gamma Neutron Activation Analysis (PGNAA) of nickel contaminated water samples was carried out. Water samples containing 2.7, 5.0, and 6.5 weight percent (wt%) of nickel were used to measure the MDC of $CeBr_3$ detector based PGNAA setup. The MDC was measured from 8993 and 9498 keV gamma rays from nickel. From the difference between the sample spectrum and background spectrum, the net nickel counts were extracted and were proportional to the nickel concentration. The integrated yield of nickel peak in each sample difference spectrum was assumed to be proportional to the nickel concentration in the corresponding sample. A linear regression was fitted between net nickel peak integrated yield and the corresponding nickel concentration in a water sample and a correlation coefficient of $R^2 = 0.997$ was obtained. The MDC was measured from the total counts of the two peaks and was found to be $0.0815 \pm 0.0250\text{ wt\%}$ which corresponds to $815 \pm 250\text{ ppm}$. This verifies the excellent performance of the $CeBr_3$ detector, for the detection of nickel in water samples.

1 Introduction

Prompt Gamma Neutron Activation Analysis (PGNAA) is a radio-analytical method, used to determine the elemental composition of materials. It is a non-destructive technique and is mainly used to detect the trace amounts of elements in the target sample. PGNAA is widely applicable in most of the scientific fields, including physics, materials science, chemistry, geology, archeology, and pharmaceutical fields. Due to continuous advancement in gamma ray detection capability such as enhanced detection efficiency and energy resolution, the applications of PGNAA technique is increasing in numerous environmental, homeland security, industrial, and medical disciplines. In most cases it is essential to measure the composition of a sample, i.e., what is the percentage of each element within a sample. Such situations often arise in testing samples for harmful radioactive or toxic contaminants in water, food, soil, and even in building materials [1]. PGNAA is an efficient technique in such situations for analyzing samples of the order of micrograms to kilograms and can be handled easily.

When the sample under consideration is bombarded with neutron beams, the elements present in the sample emit gamma rays of different energies depending upon concentration in the sample. These emitted rays are detected by the detector which converts these gamma rays into electrical pulses that can be viewed on a computer screen in form of peaks of a particular distribution. PGNAA is commonly used to detect water contamination in many industries such as petroleum, pharmacy, agriculture, and many other. In this study, PGNAA technique was used to detect nickel contamination in water. Nickel is mostly used in fabrication of stainless steel products. Nickel also used in other industries such as rechargeable batteries, catalysis, and foundry products.

Most of the time industrial wastes are in the form of liquid. If these industrial wastes are not treated properly, they may have contaminated water which causes many health effects. Some of these health effects causes due to having large quantities of nickel including highly chances of development of larynx cancer, nose cancer, prostate cancer, lung cancer, lung embolism, birth defects, respiratory failure, heart disorders, asthma, and chronic bronchitis [2]. Therefore, the monitoring of nickel concentration levels in such industrial disposal is very important for environmental issues.

Basic Principles of PGNAA

The nuclear reaction used for prompt gamma-ray activation analysis is the neutron capture (n, γ) reaction. When a neutron is absorbed by a target nucleus, the compound nucleus is in an excited state with energy equal to the binding energy of the added neutron. Then, the compound nucleus will almost instantaneously ($< 10^{-14}s$) de-excite into a more stable configuration through emission of characteristic prompt gamma rays. In many cases, this new

configuration yields a radioactive nucleus which also de-excites (or decays) by emission of characteristic delayed gamma rays. PGNA is based on the detection of the prompt gamma rays emitted by the target during neutron irradiation, while neutron activation analysis (NAA) is utilizing the delayed gamma rays from the radioactive daughter nucleus. The process of generation of prompt gamma ray is shown in Figure 1.

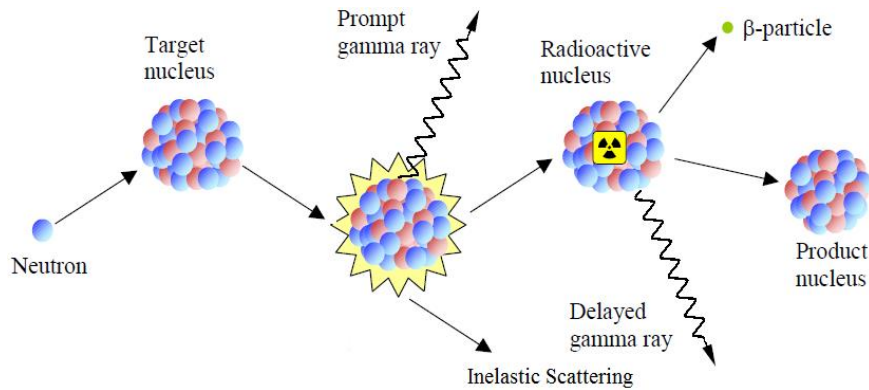
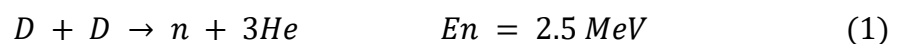


Figure 1. The process of neutron captured by target nucleus followed by the emission of prompt gamma ray, delayed gamma ray, and beta particle.

It is vital to understand the difference between PGNA and its closely-related associate, NAA. With reference to Figure 1, NAA would analyze the delay gamma rays while PGNA would study the prompt gamma rays [3]. PGNA utilizes the prompt gamma rays emitted by the excited metastable product, well before it undergoes any radioactive decay. This is the way where the final nucleus releases the excitation energy, gained in the reaction, and the time scale is of order 10^{-15} s. Hence, in cases where getting rapid results is a priority, PGNA is clearly the advantageous method. Within PGNA set-up, the neutrons are produced by a neutron generator that uses nuclear fusion of 2 deuterium atoms as per:



where by accelerating a deuteron to a few hundred *keV* of energy and hitting onto a deuterium target, fusion of deuterium atoms ($D + D$) results in the above reaction with the production of a neutron with a kinetic energy of approximately 2.5 *MeV* [4].

However, these neutrons are fast neutrons with low capture cross-section so a polyethylene moderator (having high density of atomic hydrogen) slows them down until they become slow-moving thermal neutrons. Hydrogen has almost the same mass as neutrons so linear momentum conservation ensures maximum energy loss from and slowing down of the neutrons, and thus high thermal neutron generation rate. The basic collision theory states that if a moving mass collides into a stationary mass, energy loss from the first mass is maximized if the 2 masses are the same, based on the energy-loss equation given below:

$$\frac{E_{R|max}}{E_n} = \frac{4A}{(1 + A)^2} \quad (2)$$

where A is the mass of the moderator nucleus, E_n is the energy of the incident neutron and $E_{R|max}$ is the maximum possible energy loss from the recoiling moderator nucleus. We want to maximize the ratio $\frac{E_{R|max}}{E_n}$, under which circumstance the emergent neutron has the lowest energy (and speed), thus producing thermal neutrons, and calculus yields $A = 1$ as the condition for $\frac{d}{dA} \left(\frac{E_{R|max}}{E_n} \right) = 0$. So, the condition i.e., $A = 1$ implies that the best moderator has mass number of 1, which explains why hydrogen is an ideal neutron moderator.

In the field of gamma ray detection, the primary issue is the detection of low intensity gamma-ray emissions. In such cases, amongst others, the count rate is often extremely low hence the detector should have high detection sensitivity. As compared to other detectors like, $LaBr_3:Ce$, $NaI(Tl)$, BGO, and $HPGe$, the $CeBr_3$ detector offers many advantages in terms ease-of-use and high energy resolution over all the other detectors. As shown by F. Quarati et al. [5] “ $CeBr_3$ is an optimum compromise for the detection of low intensity gamma rays.” This advantage is due to both cerium and bromine not being naturally radioactive, which makes them suitable for low and high energy applications [6]. Hence, a $CeBr_3$ detector was chosen for the present study.

2 Objectives

A large cylindrical $76\text{ mm} \times 76\text{ mm}$ (height \times diameter) $CeBr_3$ detector has been tested to detect nickel concentration in contaminated water samples. The measurement was carried out using a portable neutron generator-based PGNAA [7]. The MDC was measured for the detection of nickel in water sample.

3 Experimental setup

Figure 2 shows the PGNAA setup with the high-density polyethylene cylindrical moderator, MP320 portable neutron generator, and the $CeBr_3$ detector. The portable neutron generator-based PGNAA setup consists of a cylindrical moderator made of high density polyethylene $[(C_2H_4)_n]$. The moderator has a central cylindrical cavity that can accommodate a cylindrical specimen with a maximum diameter of 9 cm and a length of 14 cm. A cylindrical $76\text{ mm} \times 76\text{ mm}$ (height \times diameter) $CeBr_3$ gamma-ray detector, with its longitudinal axis aligned along the moderator and sample’s major axis, views the sample at a right angle to the neutron generator axis. In order to prevent undesired gamma-rays and neutrons from reaching the detector, lead and paraffin shielding were provided around the gamma-ray detector.

The MP320 portable neutron generator produce a stream of 2.5 MeV neutrons by the $D + D$ fusion reaction. A pulsed beam of 2.5 MeV neutrons was produced via the $D(d, n)$ reaction using a $70\ \mu A$ deuteron beam of 70 keV energy. At 2.5 MeV, the neutrons are fast neutrons, with small neutron capture cross-section. These fast neutrons from the generator are slowed down by polyethylene (high atomic hydrogen density) moderator to yield thermal

neutrons, which have a large neutron capture cross-section. A cylindrical cavity of radius 100 mm has been drilled through the moderator so that a cylindrical sample can be tested by PGNAA. Unwanted neutrons and stray gamma-rays are obstructed from entering the detector using 3 mm thick lead shielding and 50 mm thick paraffin shielding. The detector is high-sensitivity, $CeBr_3$ gamma-ray spectrometer supplied by Scionix Holland BV.

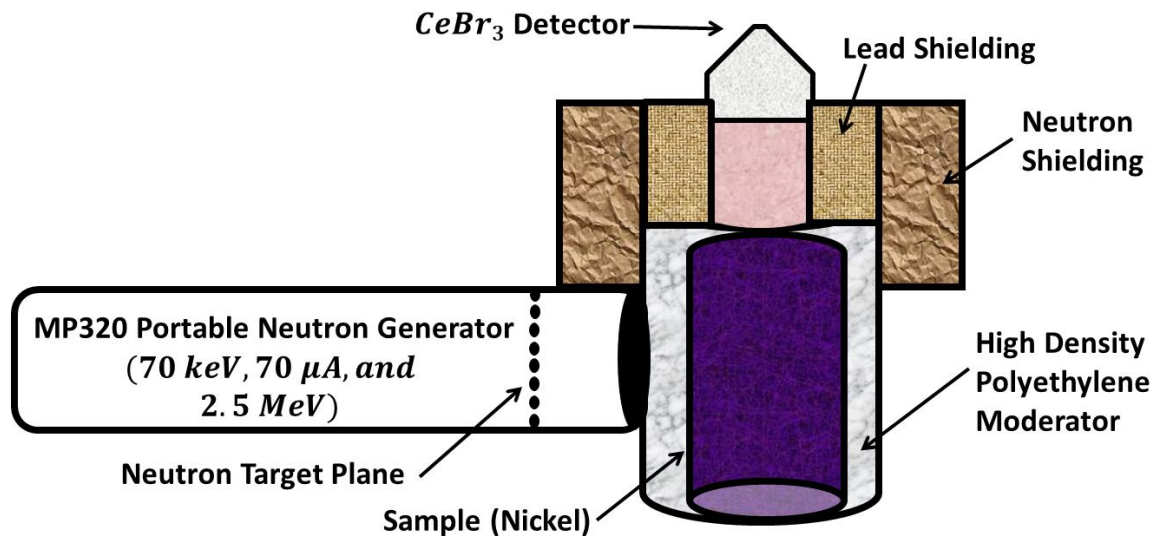


Figure 2: Schematic representation of the MP320 portable neutron generator based PGNAA setup.

The samples used in this experiment are listed in Table 1. Three nickel-contaminated water samples, present in our laboratory, prepared by the department of Chemistry, KFUPM, having 2.7, 5.0, and 6.5 wt% nickel concentrations, were used for the analysis.

Table 1: List of nickel samples used for analysis

S. No.	Chemical Solution	Molarity (mole)	Nickel Concentration (wt%)
1	$Ni(NO_3)_2$	0.5	2.7
2	$Ni(NO_3)_2$	1.0	5.0
3	$Ni(NO_3)_2$	1.4	6.5

To start the experiment, we are supposed to ensure safety to the personnel, the main experimental room (where the neutron generator is) was securely locked before switching on the neutron beam. A +700V bias voltage was applied to the detector during the experimentation. The detector was connected to preamplifier to minimize the sources of noise and convert gamma rays into electrical signals which sent to an amplifier circuit in the control room. The $CeBr_3$ detector displays the output in the form of an intensity vs channel number that is displayed on a computer. These are the general steps in our experimental set-up.

The characteristic gamma rays emitted by the sample after irradiation serve as fingerprints which is measured and counted with a specific energy to deduce the chemical element of the sample. Hence a series of electronic components, are connected to the detector. A photomultiplier and pre-amplifier are coupled to the detector to convert the incoming photon

to electrical signal and minimize the source of noise transmitted with the signal respectively. Other components include: an amplifier which increases the amplitude of the signal, an analogue to digital converter (ADC) that digitizes the input pulse height and assigns it to a specific channel, a linear gate stretcher which is to gate a signal prior to its pulse-height analysis when necessary. The prompt gamma ray data from the samples were therefore collected in a personal computer. In order to allow the energy region with maximum energy peak of 10 MeV with 512 channels the coarse and fine gains are adjusted to 5 and 11 respectively, on the amplifier of the electronic setup.

3.1 Energy Calibration of detector using Cs-137 and Co-60 Sources

The naturally-radioactive isotopes present in the detector material emit gamma rays, which constitutes the intrinsic spectrum. To measure the intrinsic spectrum of the $CeBr_3$ detector, the neutron beam was switched off, and no sample was placed in the cavity. Hence, the detector only detected the presence of naturally-occurring radioisotopes present in the detector. The run time was approximately 2998 seconds.

In general, detector spectrum shows an exponentially-decreasing intensity profile modulated with impurity radioisotope peaks, which agrees with the theoretical predictions since there is generally less random background radiation at higher energies than lower energies. However, this smoothly-decaying profile is interrupted by prominent intrinsic peaks that correspond to the decay energies of various natural radioisotopes present in the detector. From Quarati et al [5], we learn that Ce and Br elements are present in naturally occurring radioisotopes, and the reason for intrinsic activity is the actinium-227 (^{227}Ac) radioactive impurities present in the raw materials used for the detector. They attribute this contamination to the homologous nature of Ac and Ce , which makes it extremely difficult to separate them from one another, hence the cerium would be contaminated with trace amounts of actinium. According to the literature, the intrinsic spectrum of $CeBr_3$ detector has 3 prominent peaks at 1479, 1746, and 1995 keV due to ^{227}Ac contamination in the $CeBr_3$ detector as shown in Figure 3.

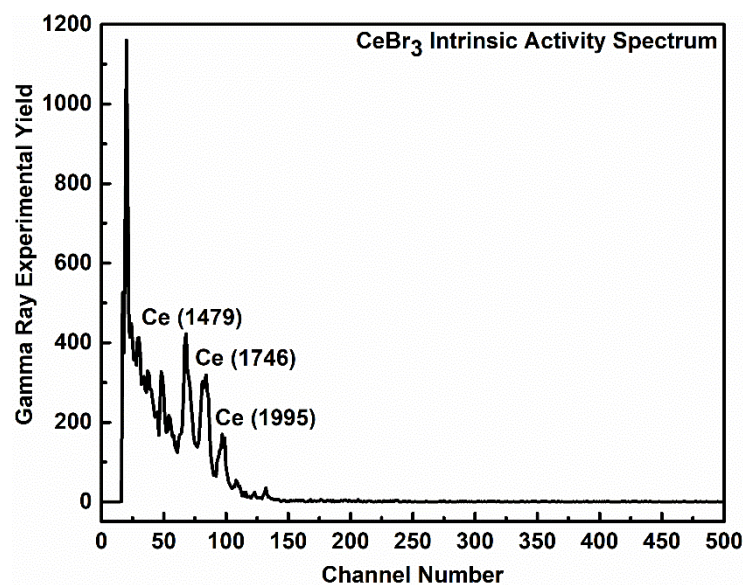


Figure 3: Detector ($CeBr_3$) intrinsic activity spectrum.

The intrinsic spectrum acquired from the $CeBr_3$ detector was originally in terms of channel number, so we have to convert those channel number into energy by calibrating with known peaks. For this purpose, Cesium-137 (Cs-137) and Cobalt-60 (Co-60) samples with known peaks were used for the energy calibration. Figure 4(a) represent the full spectrum of Cs-137 with its one characteristic peak at 661 keV and Figure 4(b) shows the full spectrum of Co-60 with its 2 characteristic peaks at 1173 and 1333 keV.

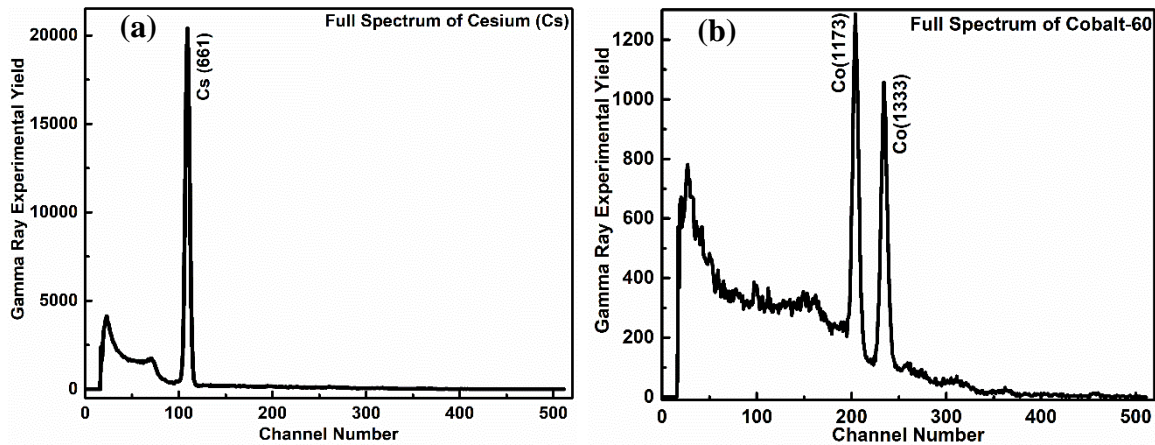


Figure 4: Full spectrum of (a) Cs-137 and (b) Co-60 for calibration with $CeBr_3$ detector.

These two known peaks of Co-60 and one peak of Cs along with their corresponding channel numbers are used in Figure 4, to derive the energy calibration ratio, which is the gradient of the best-fit line and equals $5.2759 \text{ keV/channel}$. This number was used to convert the intrinsic spectrum of the detector from channel number into an energy spectrum.

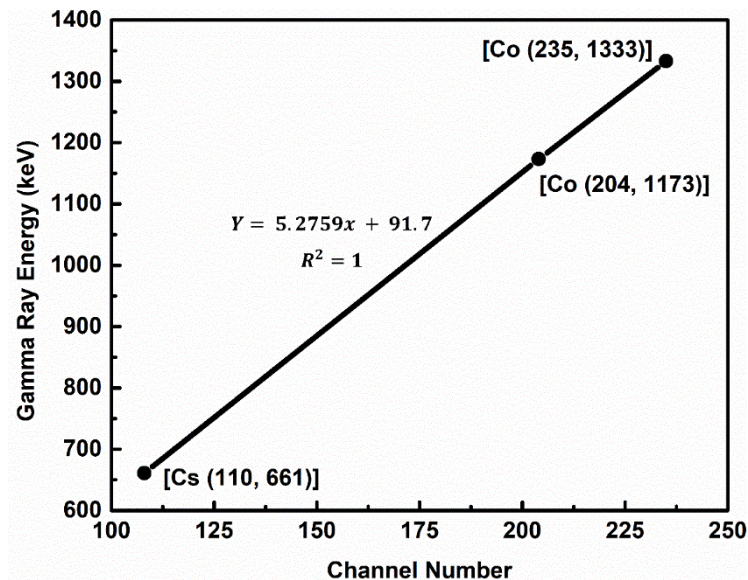


Figure 5: Energy calibration curve of the $CeBr_3$ detector using Cs-137 and Co-60 standard samples.

This is indeed observed in Figure 5, which shows intrinsic gamma ray activity spectrum of the $CeBr_3$ detector over the 0 – 2500 keV energy range. This spectrum was taken with amplifier higher gain settings (coarse gain = 20, fine gain = 8.00) that allows the full spectrum

to be recorded as the peaks of interest are in the low-energy region at 1479, 1746, and 1995 *keV* as shown in Figure 6.

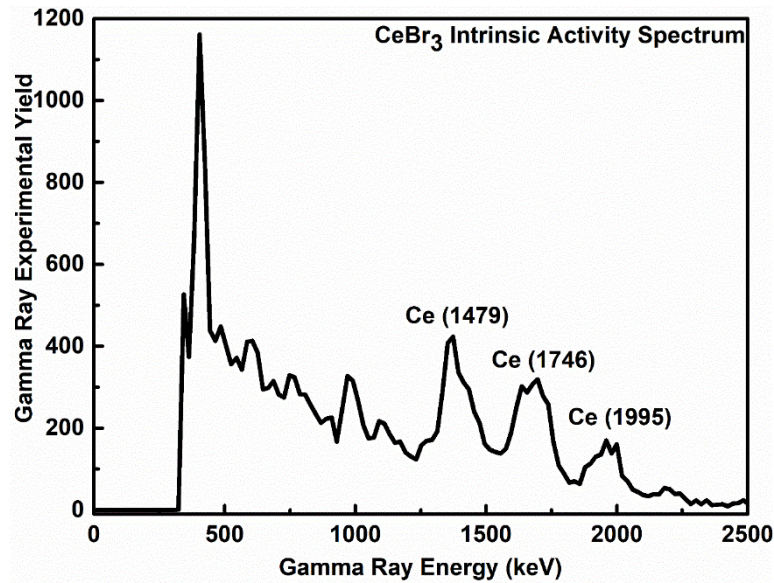


Figure 6: Detector (*CeBr₃*) intrinsic activity spectrum.

4 Prompt Gamma Ray Studies

The above calculation and discussion was about the low energy calibration of *CeBr₃* detector, but we are equally interested in high energy calibration. Because the prominent peaks of our sample (Ni) lies at high energy, in the range of 8900 to 9500 *keV* [8]. Therefore, a calibration was needed to obtain the relation between channel number and the energy of gamma rays, at this high range, but as there is no available standard sample at the required high energy range. For this reason, a calibration was performed by fitting the gamma ray peak of the known element in the moderator, i.e., Hydrogen. The hydrogen that was detected came from the polyethylene (C_2H_2)_n moderator.

4.1 Background Spectrum

It is known that the gamma rays energy of hydrogen is 2223 *keV* [8]. Therefore, the high energy activation measurement of the detector was taken with low coarse gain 5 and fine gain 11 of the amplifier to bring this marker peaks at low energy and to enlarge the high energy range. From the raw data it was observed that hydrogen peak (2223 *keV*) was located at channel number 110, as shown in Figure 7. From here, we can find the relation between channel number and the gamma rays energy.

$$\text{Energy per channel} = \frac{2223 \text{ keV}}{110} = 20.2 \text{ keV}$$

we obtained that, 1 *channel* = 20.2 *keV*. Having this relation, all spectrum with respect to the channel number were converted into spectrum with respect to the energy. The spectrum exhibits the full channel numbers along with associated marker peak of hydrogen (2223*keV*) at channel number 110 is shown in Figure 7.

4.2 Nickel-Contaminated Water Sample Spectrum

To measure the sample spectrum of the nickel-contaminated water samples, the bottle was inserted into the moderator cavity and the neutron beam was switched on. In this case, the net Ni peaks get superimposed on the background spectrum to give the net sample spectrum.

The experimental run time of the detector activation spectrum and net sample spectrum must correspond with each other. For instance, our former run time was 2998s, in which case the latter must also be approximately 2998s. Otherwise, if the background is run much longer/shorter than the samples, the background will naturally be higher/lower than the net nickel spectra, and we will get a net depression instead of peaks. Figure 7 shows a nickel spectrum (6.5 wt%) superimposed upon a background spectrum. The region of interests shows the effect of the nickel sample having two prominent peaks at 8993 and 9498 keV in response of the moderator peak at 2223 keV.

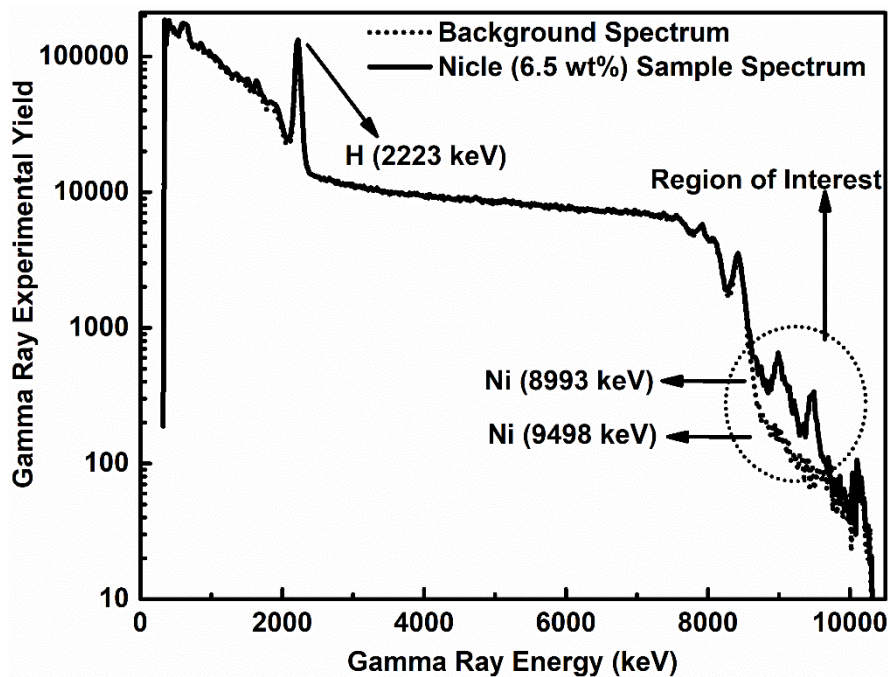


Figure 7: Superimposed spectra of the background (dotted line) and nickel (solid line).

In Figure 7, we can see all elements detected gamma rays spectra. It shows that the elements come not only from the sample but also from the detector and moderator. These other peaks that contributing to the spectra are considered as the background peaks. Subsequently, prompt gamma ray spectra were recorded for three nickel-contaminated water samples, having 2.7, 5.0, and 6.5 wt% nickel concentrations.

5 Results and Discussion

As shown in Figure 8, the spectrum from each sample with different concentration of nickel were normalized and then compared to each other. Form this result we can see that all the three samples of Ni are having two broad peaks at 8993 keV and 9498 keV, while the background spectrum is completely flat in the region of interest, having no contribution to the desired peaks.

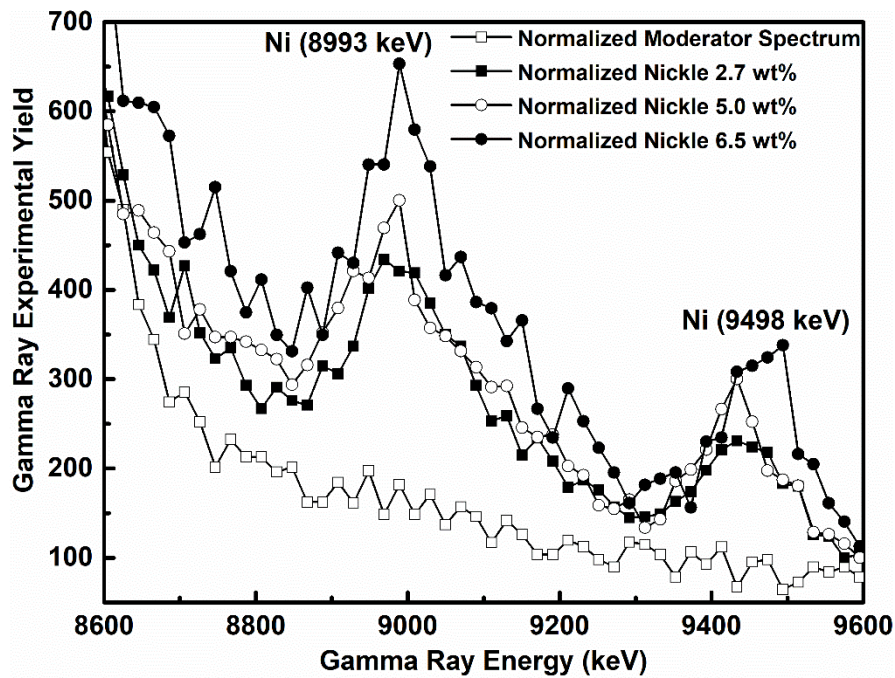


Figure 8: Normalized Spectra for the three nickel samples with 2.7, 5.0, and 6.5 wt% nickel concentration.

We analyzed the difference spectra to remove the background effect and to determine whether the detector is performing reliably. To extract the difference spectra, the detector background spectrum is subtracted from the sample spectrum. The background free spectra of all the three samples having 2.7, 5.0, and 6.5 wt% nickel concentrations were superimposed upon each other over a gamma ray energy range in the region of interest i.e., 8600 – 9600 keV. Figure 9 shows the difference spectra of the nickel samples.

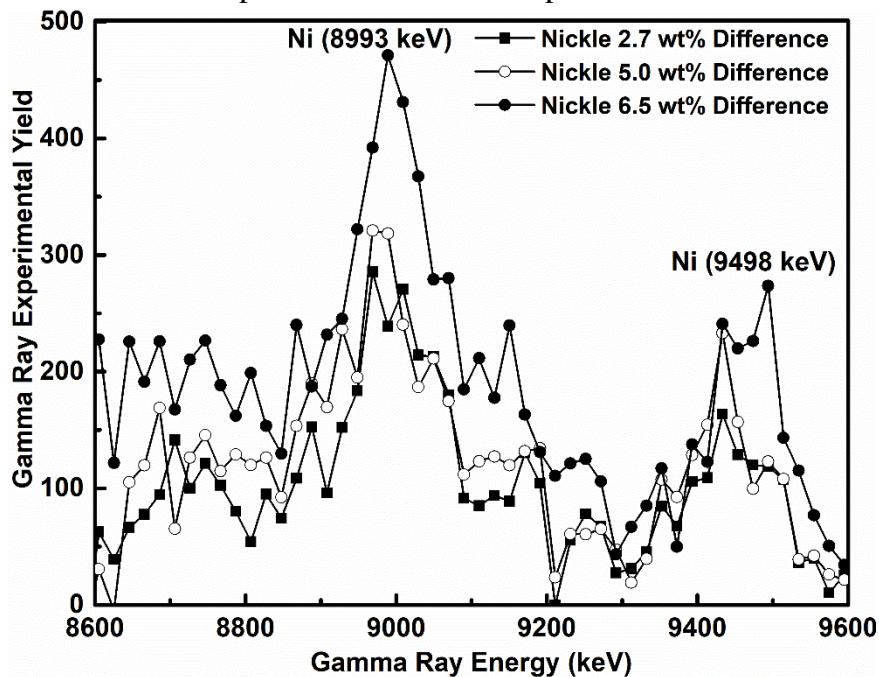


Figure 9: Difference spectra for three nickel samples with 2.7, 5.0, and 6.5 wt% nickel concentration.

The area under these three difference spectra gives the integrated yield, which is theoretically proportional to the nickel concentration in the water samples. Next, we plot the integrated yield against nickel concentration in Figure 10 to determine, whether our detector gives the linear relationship. The least-squares regression line of integrated yield against nickel

concentration is illustrated in Figure 10 with a regression equation of $y = 204x + 915$ and a correlation coefficient of $R^2 = 0.9979$.

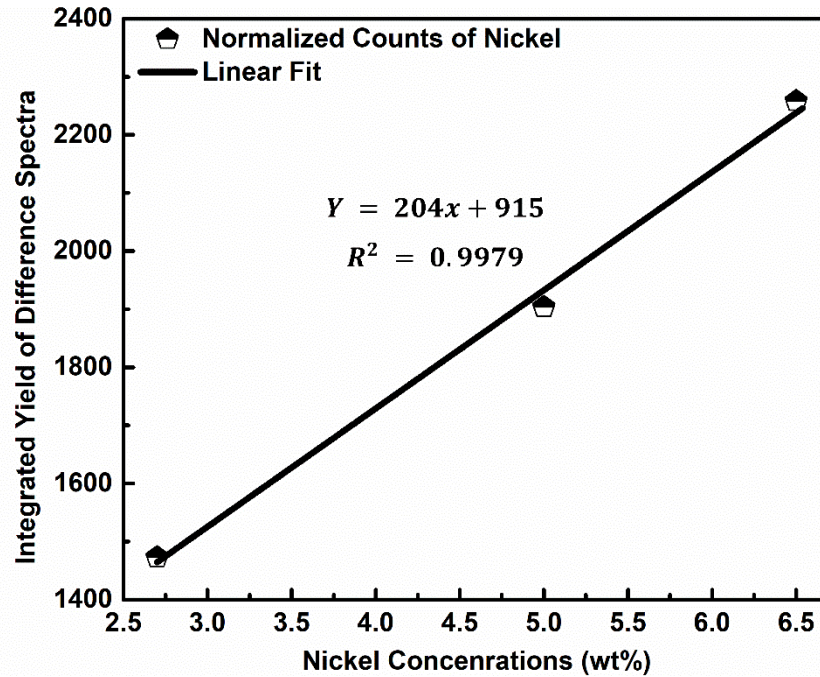


Figure 10: Concentration calibration plot of gamma-ray intensity vs. nickel concentrations (wt%).

Analyzing Figure 10 more clearly, we notice that the 3 data points display a good scatter about the best-fit line, as evidenced by the points being close to the best fit regression line. This is an indication that only random errors (which are uncontrollable and cannot be eliminated) are affecting the data. Another indication is that the correlation coefficient of 0.9979 implies a very strong positive relationship between the two sets of data. Since our experimental data agree with the theoretical proportionality relationship, we have verified that the $CeBr_3$ detector is working reliably.

5.1 Minimum Detection Limit of Nickel in Water Samples

The minimum detection limit (MDC) of nickel in water was calculated for the KFUPM PGNA setup using $CeBr_3$ detector. The procedure of MDC have been discussed by DA Gedcke et al [9], and can be calculated by using the following equation.

$$MDC = 4.653 \times (C/P) \times \sqrt{B} \quad (3)$$

where, C represents the concentration in wt%, P represents the net counts under the peak, and B represents the associated background counts under the peak.

The error in MDC was calculated from equation 4.

$$\sigma_{MDC} = \left(\frac{C}{P}\right) \times [\sqrt{(2 \times B)}] \quad (4)$$

The MDC of nickel in the water samples for the KFUPM PGNNA setup was calculated for 8993 keV and 9498 keV gamma rays from the nickel in the samples. The MDC limit of nickel in water samples was separately calculated for each peak and then was combinedly calculated for both the peaks (because these two peaks are from the same isotope). The final

MDC of nickel in water was obtained as $0.0815 \pm 0.0250 \text{ wt}\%$ which corresponds to $815 \pm 250 \text{ ppm}$. The details of MDC are given in the Table 2.

Table 2: MDC values for the two peaks of nickel and combined.

Peak No.	MDC (wt%)	MDC (PPM)	mole	wt%	P	B
8993 keV	0.0946	945.91	0.5	2.7	1473	123
	0.1636	1635.78	1	5.0	1513	115
	0.2915	2915.37	1.4	6.5	1012	94
9498 keV	0.1556	1556.16	0.5	2.7	713	78
	0.3011	3011.05	1	5.0	558	53
	0.4713	4712.71	1.4	6.5	452	49
8993 keV + 9498 keV (Combines)	0.0815	814.79	0.5	2.7	2186	201
	0.1445	1444.41	1	5.0	2071	168
	0.2486	2485.64	1.4	6.5	1464	143

6 Conclusion

PGNAA technique has been employed to find the relation between nickel concentration in water solution and the number of gamma rays detected by $CeBr_3$ detector. The measurements were carried out with water samples containing 2.7, 5.0, and 6.5 wt% of nickel.

It was found that, higher concentration of nickel, resulting more number of gamma rays. We have verified the performance of $CeBr_3$ detector by comparing its performance against a theoretical principle, which states that the integrated prompt-gamma yield is proportional to the concentration of the sample tested. It was concluded from the linear regression curve fitting of the sample that the detector acts in compliance with the aforesaid principle, thereby proving the reliable performance of $CeBr_3$ detector. The calculated MDC for the nickel was $0.0815 \pm 0.0250 \text{ wt}\%$ which corresponds to $815 \pm 250 \text{ ppm}$. Lastly, the technique used in this report can be exploited for the detection limit of any detector, and also for elemental characterization of unknown samples, which is useful in environmental pollutants and illegal materials testing, thereby demonstrating that this technique can have beneficial consequences for humanity.

7 Acknowledgements

I would like to thank my course supervisor Professor Akhtar Abbas Naqvi for dedicating most of his time to make me understand the basic principles behind the PGNAA set up and for his methods of correcting mistakes with sublime encouragement. Also, gratitude must be offered to Mr. Rashid, the engineer – always willing to help and was extremely patient in answering our repeated requests for operating the neutron gun.

8 References

1. A. Naqvi, et al., *Multiple Gamma-Ray Detection Capability of a CeBr₃ Detector for Gamma Spectroscopy*. Journal of Spectroscopy, 2017. **2017**.
2. E. Denkhaus and K. Salnikow, *Nickel essentiality, toxicity, and carcinogenicity*. Critical reviews in oncology/hematology, 2002. **42**(1): p. 35-56.
3. D. Williams, et al. *High Intensity, Pulsed, D-D Neutron Generator*. in *AIP Conference Proceedings*. 2009. AIP.
4. W. James, et al., *Application of prompt gamma activation analysis and neutron activation analysis to the use of samarium as an intestinal marker*. Journal of Radioanalytical and Nuclear Chemistry, 1984. **83**(2): p. 209-214.
5. F. Quarati, et al., *Scintillation and detection characteristics of high-sensitivity CeBr₃ gamma-ray spectrometers*. Nuclear Instruments and Methods in Physics Research Section A: Accelerators, Spectrometers, Detectors and Associated Equipment, 2013. **729**: p. 596-604.
6. A. Naqvi, et al., *Performance tests of a large volume cerium tribromide (CeBr₃) scintillation detector*. Applied Radiation and Isotopes, 2016. **114**: p. 50-56.
7. J. Fantidis, et al., *The comparison of four neutron sources for Prompt Gamma Neutron Activation Analysis (PGNAA) in vivo detections of boron*. Journal of radioanalytical and nuclear chemistry, 2011. **290**(2): p. 289.
8. A. Naqvi, et al., *Pulse height tests of a large diameter fast LaBr₃: Ce scintillation detector*. Applied Radiation and Isotopes, 2015. **104**: p. 224-231.
9. D. Gedcke, *How counting statistics controls detection limits and peak precession*. ORTEC Application Notes AN59. Website:/www.ortec-online.comS, 2001.